The RING network: improvements to a GPS velocity field in the central Mediterranean

Antonio Avallone[1,*], Giulio Selvaggi[1], Elisabetta D'Anastasio[1], Nicola D'Agostino[1], Grazia Pietrantonio[1], Federica Riguzzi[1], Enrico Serpelloni[1], Marco Anzidei[1], Giuseppe Casula[2], Gianpaolo Cecere[1], Ciriaco D'Ambrosio[1], Prospero De Martino[3], Roberto Devoti[1], Luigi Falco[1], Mario Mattia[4], Massimo Rossi[4], Francesco Obrizzo[3], Umberto Tammaro[3], Luigi Zarrilli[1]

[1]*Istituto Nazionale di Geofisica e Vulcanologia, Centro Nazionale Terremoti, Roma, Italy*

[2]*Istituto Nazionale di Geofisica e Vulcanologia, sezione di Bologna, Italy*

[3]*Istituto Nazionale di Geofisica e Vulcanologia, sezione di Napoli, Italy*

[4]*Istituto Nazionale di Geofisica e Vulcanologia, sezione di Catania, Italy*

Article history
Received January 18, 2010; accepted April 15, 2010.
Subject classification:
Geodesy, Seismotectonics, CGPS network, GPS data analysis, Central Mediterranean

ABSTRACT

Since 2004, a continuous Global Positioning System (GPS) network has been operated by the Istituto Nazionale di Geofisica e Vulcanologia (INGV) to investigate active tectonic processes in Italy and the surrounding regions, which are still largely debated. This important infrastructure is known as Rete Integrata Nazionale GPS (RING) network, and it consists of about 130 stations that are deployed all over Italy. The development and realization of a stable GPS monumentation, its integration with seismological instruments, and the choice of both satellite and internet data transmission, make this network one of the most innovative and reliable CGPS networks in the world. The technologically advanced development of the RING network has been accompanied by the development of different data processing strategies, which are mainly dependent on the use of different GPS analysis software. The different software-related solutions are here compared at different scales for this large network, and the consistency is evaluated and quantified within an RMS value of 0.3 mm/yr.

Introduction

The plate boundary between Nubia and Eurasia is characterized by complex kinematics, mainly due to geometrical and rheological features that remain to be described in detail [Westaway 1990, Serpelloni et al. 2005]. Several seismotectonics syntheses have been proposed over the last two decades, both at local and regional scale [Anderson and Jackson 1987, Jackson and McKenzie 1988, Ekstrom and England 1989, Westaway 1990, Serpelloni et al. 2005, D'Agostino et al. 2008]. The plate boundary shows a transition from simple deformation at the oceanic plate boundaries of the Atlantic, which is characterized by narrow seismic belts, to a broad zone of seismicity and deformation that characterizes the Apennines and Alpine belts, which results in a complex pattern of crustal stress and strain. The distribution of the instrumental seismicity (Figure 1) indicates the high crustal fragmentation of the area and outlines a first-order picture of the plate boundary mosaic. Here, several quasi-aseismic domains, such as the Adriatic Sea and the Tyrrhenian Sea, are embedded in domains with higher seismicity where most of the deformation probably occurs.

The GPS is a fundamental tool for studying the kinematics of continental deformation at diffuse plate boundaries, which allows inter-seismic velocities and velocity gradients at different scales to be measured. The evaluation of the instantaneous velocities of most of the tectonic plates has become increasingly well constrained due to improvements in the global tracking network and the GPS infrastructure (i.e. the increasing number of continuously operating stations worldwide, which allows better resolution of the global reference frame). Various estimates of GPS-derived Africa-Eurasia Euler vectors have been proposed from the analysis of space geodetic data [Sella et al. 2002, Calais et al. 2003, Kreemer et al. 2003, McClusky et al. 2003, D'Agostino et al. 2008]. The short-time span and the lack of density prevent those works to adress the question of the deformation inside the plate boundary itself, or allow just the identification and discussion of the behaviour of relatively large blocks. An example is the definition of an Adriatic plate and its southern boundary [Calais et al. 2002, Oldow et al. 2002, Battaglia et al. 2004] and the present-day activity of the Calabrian slab [Goes et al. 2004, D'Agostino and Selvaggi 2004, Chiarabba et al. 2005, Serpelloni et al. 2005]. Some recent papers [Hollenstein et al. 2003, D'Agostino and Selvaggi 2004, Serpelloni et al. 2005] indicate that strain rates in Italy are higher than expected [Anzidei et

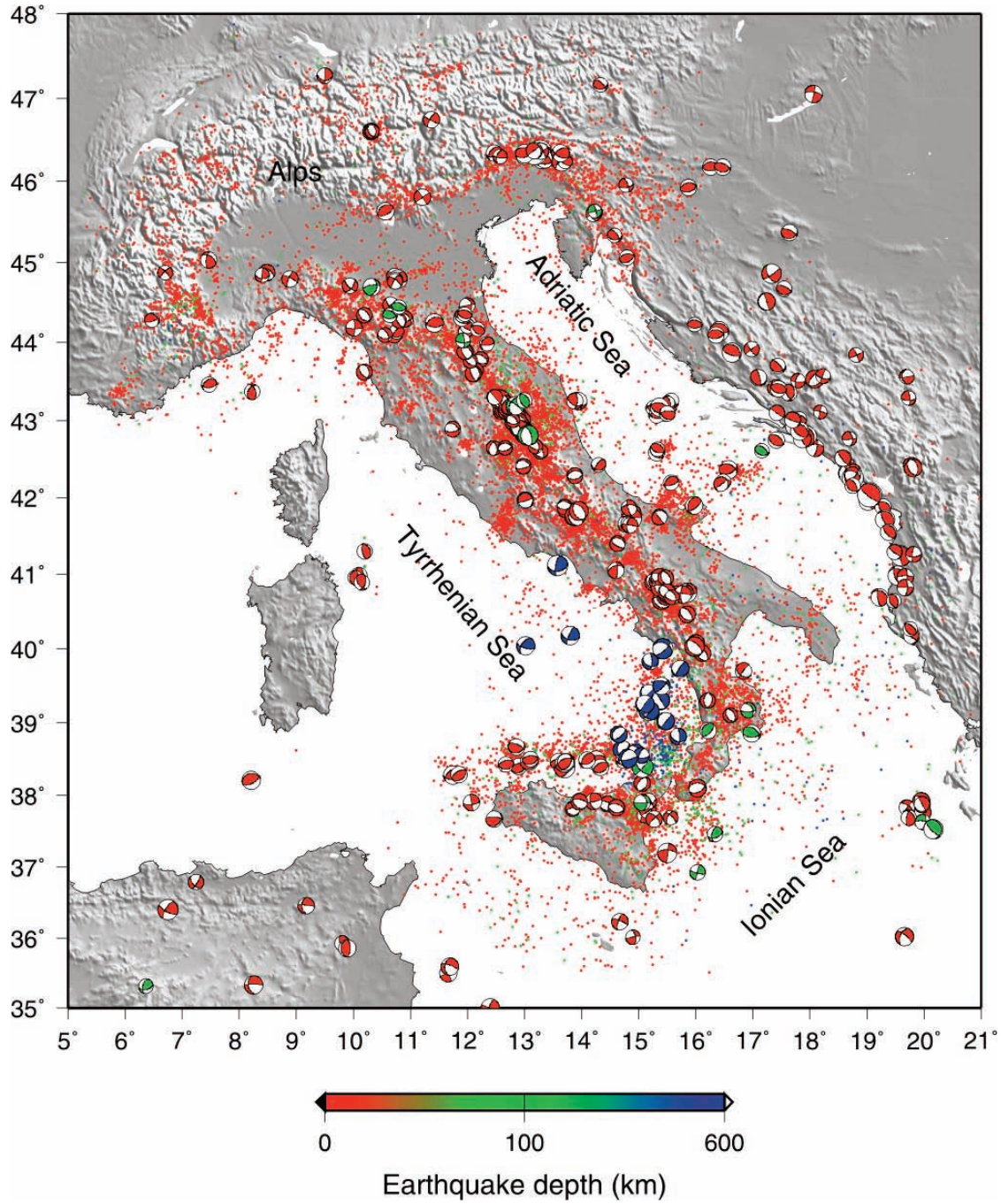

Figure 1. Seismicity distribution in the central Mediterranean. RCMT focal mechanisms from Pondrelli et al. [2004] are shown together with the 1973-2006 seismicity from NEIC (http://neic.usgs.gov). The color scale indicates the distribution of both focal mechanisms and seismicity with depth.

al. 2001], with values in the range $0.5 \div 2^{\star}10^{-7}$ yr^{-1} through Sicily and the Apennines [D'Agostino and Selvaggi 2004]. Recently, D'Agostino et al. [2008] and Devoti et al. [2008] have proposed more refined models of the active tectonics in the central Mediterranean, showing the importance of a dense CGPS network, to properly measure strain rates within the plate boundary.

The contribution of geodesy to seismological studies is also becoming more important, from the observation of the inter-seismic strain accumulation across active faults, to the constraints of the history of earthquake rupture process. The mentioned scientific topics relating to active tectonics, along with the Africa-Eurasia plate boundary zone, were the main goals for planning the dense, continuously operating, real-time Integrated National GPS (RING) network in Italy, following the examples of Japan (Miyazaki et al., 1994) and the USA [Zhang et al.1997; or http://pboweb.unavco.org].

After a first description of the aspects related to the implementation of the RING network, the aim of this study is to describe the different software-related GPS data processing strategies, and to evaluate the consistency among the different solutions, thus, finally, outlining the results carried out with the present-day GPS velocity field along with the Africa-Eurasia plate boundary zone.

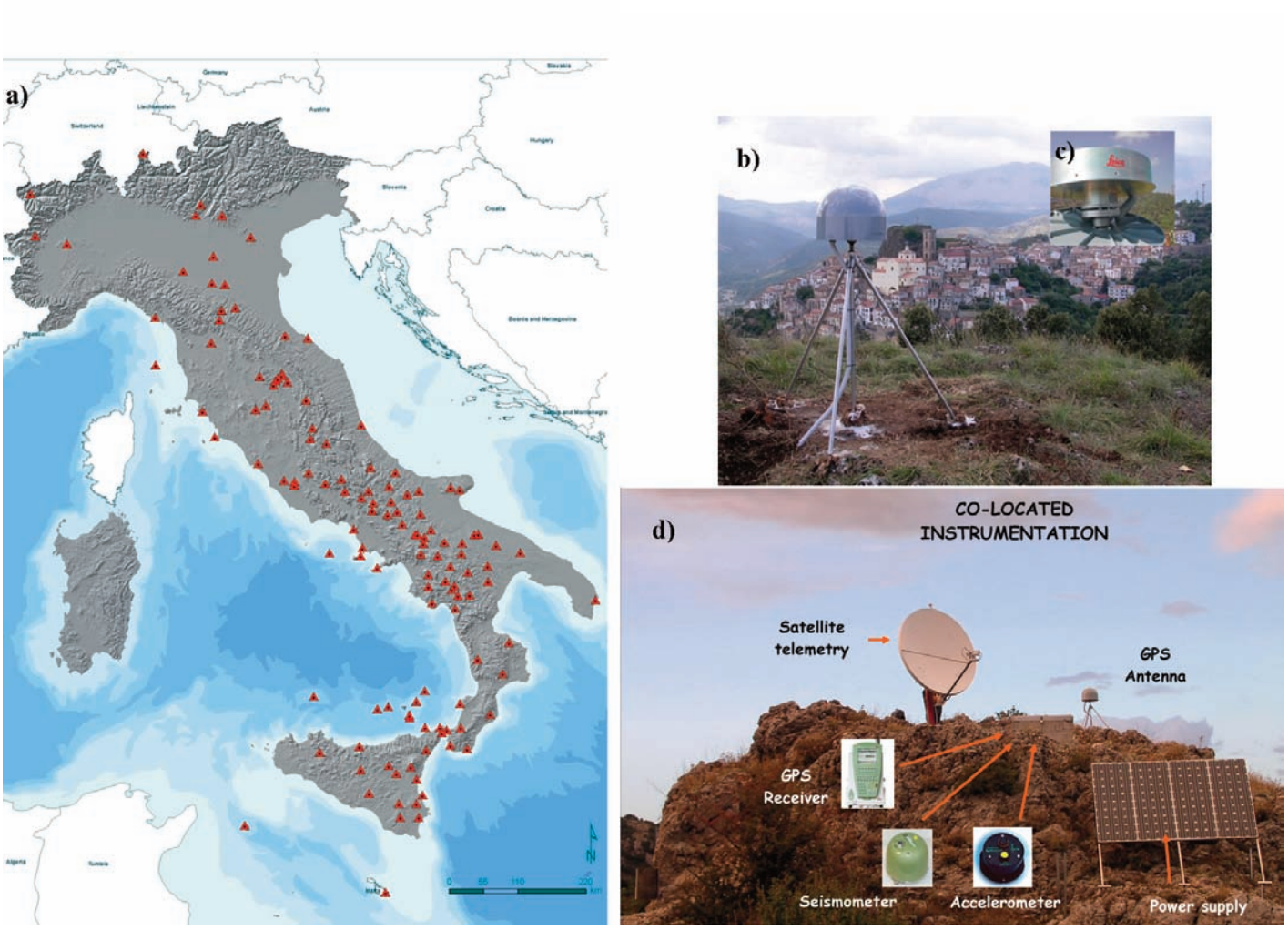

Figure 2. Details of the RING network and the RING infrastructure implementation: a) map showing the locations of all the RING network sites; b) example of short-drilled steel rod tripods adopted for use in most of the RING sites; c) details of the antenna-SCIGN mount-SCIN radome coupling; d) example of a remote RING site (SIRI) with satellite data transmission and seismic instruments co-location.

The RING network implementation

The RING network (http://ring.gm.ingv.it) has been developed in Italy since 2005 [Selvaggi et al. 2006], and it integrates various experties acquired by the INGV since the early 90s in the management of GPS networks and data [Anzidei et al. 2008]. This integration is not limited to geodesy and most of the RING stations are co-located with a seismic station including broad-band and very broad-band (40sec÷240sec) seismometers and strong motion accelerometers. The co-location of those different instruments represents a unique scientific opportunity for recording and evaluating the whole range of frequencies of the plate boundary deformation and earthquake cycle at the same site. This will allow a large range of scientific problems to be tackled, from earthquake source studies to regional plate kinematics. Moreover, the co-location of different instruments allows the use of the same transmission vector for different data types in real time, with the consequence that there will be strong cost reductions in the management of the network. The RING is thus a multi-sensor network, that transmits in real time, consisting of about 130 stations (Figure 2a). These stations are not homogeneously distributed all over Italy and their present distribution mainly reflects the results of some important projects that have been carried out (i.e. the CESIS project for southern Italy, http://www.gm.ingv.it).

In addition to the conventional monumentation types used in permanent GPS sites devoted to geophysical applications (i.e. concrete pillars on bedrock, vertical steel rod on a building), a significant effort has also been put into the development of a SCIGN-like (Southern California Integrated GPS Network, http://csrc.ucsd.edu/howTo/scignMonumentInfo.html) short or deep-drilled braced tripod, which is fastened directly to the ground and has the antenna phase center very close to the most stable point of the monumentation, i.e. at the junction of the braces (Figure 2b) [D'Ambrosio 2007]. The long-term and short-term stabilities of such a monumentation type is particularly important because of the possibility of detecting low-amplitude deformation rates, as inter-seismic or post-seismic signals.

The majority of the GPS instruments are Leica (SR520, GRX1200PRO and GRX1200GGPRO), with Chock-Ring antennae (AT504 or AT504GG). The SCIGN or SCIGN-like

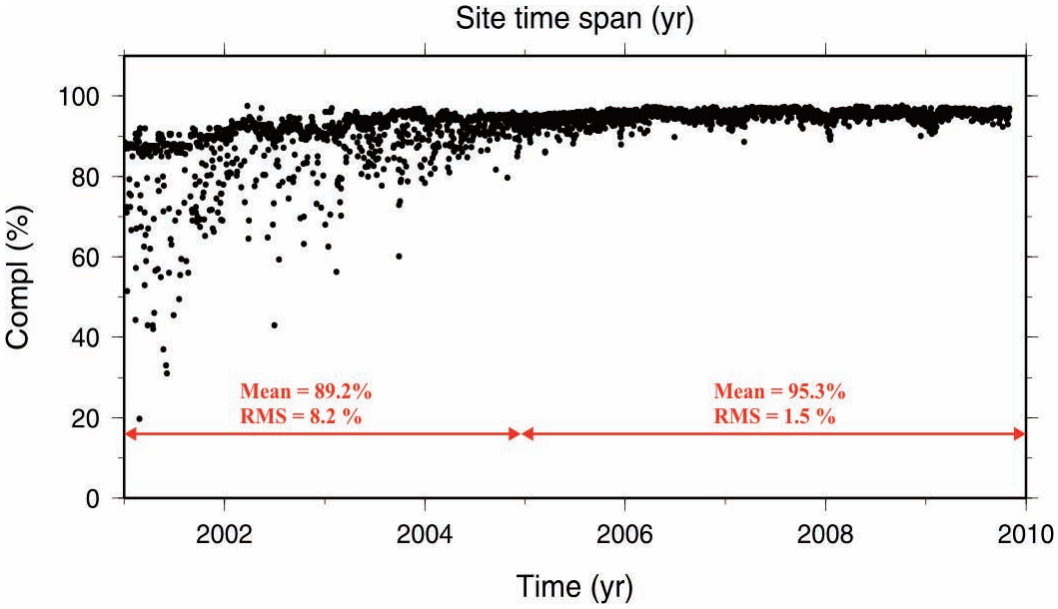

Figure 3. The *Compl* parameter evolution over time (see text) for the RING network infrastructure.

mounts are important accessories of the RING stations, and they allow a very good coupling between the antenna and the monumentation, and with the SCIGN or Leica radomes [Figure 2c].

Most of the RING sites transmit data by satellite telemetry (Nanometrics VSAT technology, http://www.nanometrics.ca) [Figure 2d]. This transmission system has the following advantages: 1) it assures optimal continuity of the observation acquisitions; 2) it allows installation of stations in remote locations that transmit both seismic and geodetic data in real time; 3) it is reliable, and provides re-transmission of lost packets; 4) it requires low power supply; and finally, 5) it allows an important reduction in management costs. The data are transmitted to three different acquisition centers (located in Rome, Grottaminarda and Catania) to assure redundancy in the satellite data acquisition of all of the RING sites. Moreover, further developments in data transmission have been carried out using both mobile phone (GPRS/UMTS) [Falco 2008] and Wi-Fi technology. These last developments are designed to ensure alternative and reliable real-time data transmission for most of the RING sites via the Internet. In conclusion, both the satellite telemetry and the internet connections currently allow for real-time transmission from about 90% of the RING sites. The real-time monitoring of the remote RING sites and the relative data acquisition are performed at the Grottaminarda INGV acquisition center, where all of the raw data are stored and archived.

A quality check of the acquired data (e.g. marker name, cycle slips, gaps, first and last epoch, acquisition percentage) is also performed using a home-made program, known as *Clinic*, based on teqc software [http://facility.unavco.org/software/teqc/teqc.html; Estey and Meertens 1999]. The resulting quality check summary is continuously stored in a database. To attest the good quality of the whole RING network infrastructure, we define a parameter for the «completeness degree» (named *Compl*) of the acquired data (Figure 3). This parameter is an average value calculated for each day, and it is obtained using the following formula:

$$Compl = \sum_{i=1}^{n} \left[\left(A_{obs} / E_{obs} \right) * \left(Hr/24 \right) \right] / n$$

where A_{obs} and E_{obs} correspond to the numbers of acquired daily observations and of expected daily observations, respectively, as they output from the teqc quality check, *Hr* represents the acquired data time-span for each rinex file, and *n* is the total number of rinex files available each day. The evolution of the *Compl* parameter with time shows a first period that lasted to approximately 2005 (i.e. before the recent developments of the RING network), which was characterized by moderate *Compl* values, with mean and RMS values of about 89% and 8, respectively. Since 2004, the RING network has guaranteed a better and optimal level of data completeness (mean = 95%; RMS = 1.5). This optimal result is mainly related to the improvements obtained using new instrumentation, and the more reliable and technologically advanced data transmission types, with respect to the conventional phone connections.

A collaborative environment has been developed to create an advanced technological frame that is devoted to complete managing and sharing of RING rinex data and of the relative information content [Cecere 2007]. This uses the recent «knowledge management» techniques [Kim et al. 2002] with the database subdivided into three levels: 1) the data, containing the raw and rinex data in a file system structure, and all of the metadata with the information of each site (i.e. logfiles, monographs, sites photos, rinex quality check summaries); 2) the data managing software

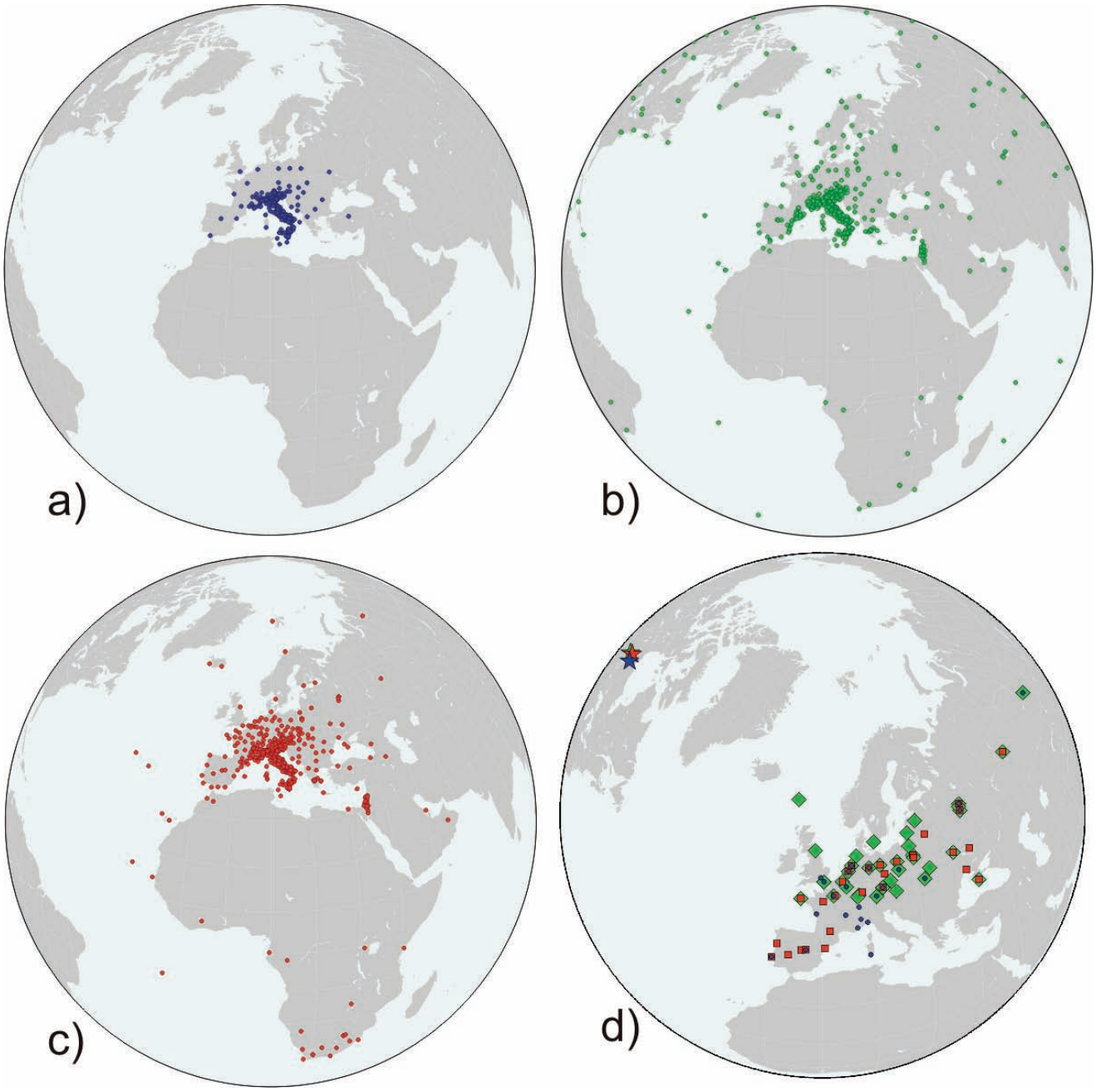

Figure 4. Maps showing the location of all of the CGPS sites used by: a) the Bernese solution; b) the Gamit solution; and c) the Gipsy solution. d) Map showing the locations of the CGPS sites defining the Eurasian reference frame in the three solutions: Bernese (blue diamonds), Gamit (green diamonds) and Gipsy (red diamonds). The location of the three Eulerian poles of the differently defined Eurasia reference frames are also shown with their associated 95% confidence ellipses (details listed in Table 1).

(i.e. *Clinic*), to check the data and to provide alerts about critical discrepancies or data gaps; 3) the web services (i.e. the RING web site, http://ring.gm.ingv.it, the RING WebGis, http://labgis.gm.ingv.it/, and the RING *Bancadati restricted area*, http://bancadati.gm.ingv.it), which allow any user to view and download dynamically created products, such as thematic maps, station log-files, monographs, quality check graphs, and coordinate time-series plots. These web services have been planned to promote data, information and knowledge exchange (know-how), starting from the point of view that the best resource for an institute is represented by the knowledge owned and shared by the people who work in it.

GPS data processing

At the INGV, the GPS data analysis is carried out with the three main geodetic-quality softwares used in the GPS scientific community: Bernese (http://www.bernese.unibe.ch/), which was developed at the Astronomic Institute of the University of Berne (AIUB); GAMIT (http://www-gpsg.mit.edu/~simon/gtgk/), which was developed at Massachusetts Institute of Technology (MIT); and Gipsy/OASIS II (http://gipsy.jpl.nasa.gov/orms/goa), which was developed at the Jet Propulsion Laboratory (JPL).

Soft.	Organization	Orbits & EOP	Elevation cutoff	Phase Centre Calibrations	Troposphere models	ZTD est. rate	Time series analysis	Reference frame transformations
Bernese	clustered	fixed	15°	relative	dry Niell + wet Niell	1hr	velocity+ annual signals + offsets	8 parameters (scale, translations & their derivatives)
GAMIT	clustered	estimated	10°	absolute	dry GMF+ wet GMF+ horiz. gradients	1hr	velocity + annual and semiannual signals + offsets	7 parameters (scale, rotations & translations)
Gipsy	Unique cluster (ambizap)	fixed	15°	relative	dry Niell + wet Niell+ horiz. gradients	5min	vel+ annual and semiannual signals + offsets	7 parameters (scale, rotations & translations)

Table 1. Comparison of the main aspects concerning the different GPS data-processing strategies.

In this section, we describe the different strategies adopted to obtain the velocity field solutions with the three softwares. The main aspects of these strategies are summarized in Table 1, to highlight the choice of similar or different models and/or parameters.

Bernese data-processing strategy

The GPS phase data are processed by subdividing the whole network into 12 regional clusters of about 40 stations each, which contain at least 11 common anchor sites, i.e. selected sites used as core sites for the cluster combination, based on station performance and geographical distribution [Figure 4a]. The GPS observations considered in this analysis span a time interval of 12 years (1998.0-2009.0). The data processing is performed by the Bernese Processing Engine of the software Bernese 5.0 [Beutler et al. 2007], which forms double difference observables. The GPS orbits and the Earth orientation parameters are fixed to the combined International GPS Service (IGS) products, and an *a-priori* error of 10 m is assigned to all of the site coordinates. The pre-processing phase that is used to clean up the raw observations, is carried out in a baseline by baseline mode. Independent baselines are defined by the criterion of maximum common observations. The elimination of gross errors and cycle slips, and the determination of new ambiguities are computed automatically using the triple-difference combination. The *a-posteriori* normalized residuals of the observations are also checked for outliers. These observations are marked for the final parameter adjustment. The elevation-dependent phase center corrections are applied, with the inclusion in the processing of the IGS phase center calibrations (relative calibrations). The troposphere modelling consists of an *a-priori* dry-Niell model that is fulfilled by the estimation of zenith delay corrections at 1-h intervals at each site, using the wet-Niell mapping function [Niell 1996]. The ionosphere is removed by applying the ionosphere-free linear combination of $L1$ and $L2$. The ambiguity resolution is based on the Quasi-Ionosphere-Free baseline-wise analysis [Beutler et al. 2007]. The final network solution is solved with back-substituted ambiguities, if they are integer; otherwise, ambiguities are considered as real-valued measurement biases. Each daily solution was estimated within a loosely constrained reference frame that is close to the rank deficiency condition, which obtains the so-called loosely constrained solution. Each solution is realized in an intrinsic reference frame that is defined by the observations themselves, and which differ from day to day only for rigid network translations, keeping the site inter-distances always well determined. In this way, the constraints to realize the chosen reference frame are imposed only a posteriori at the final stage of the analysis. The daily loosely constrained cluster solutions are then merged into global daily loosely constrained solutions of the whole network, applying a classical least-squares approach [Bianco et al. 2003]. The velocity field is estimated directly from the loosely constrained time series of the daily coordinates, obtaining a loosely constrained velocity solution. The velocities are estimated simultaneously, together with annual signals and sporadic offsets at epochs of instrumental changes. Subsequently, the loosely constrained velocity field has been transformed into the ITRF2005 reference system [Altamimi et al. 2007] by applying an eight-parameter Helmert transformation (scale, translation, and their derivatives) and the inner constraints to the final solution. The rigid plate motion is estimated directly from the official ITRF2005 velocity solution, and it is statistically inferred using simple χ^2 test-statistics iteratively applied to select the coherent subset of sites that define a stable plate [Devoti et al. 2008]. Starting from three central European sites (the pilot-triad: WSRT, WTZR and ZIMM), a total of 24 sites were assigned to a stable plate, with $\chi^2_\nu = 1.46$. The absolute ITRF2005 Eurasia pole and rotation rate are (55.85° N, 95.72° W) and $(0.266 \pm 0.003)°$/Myr, which are consistent with previous

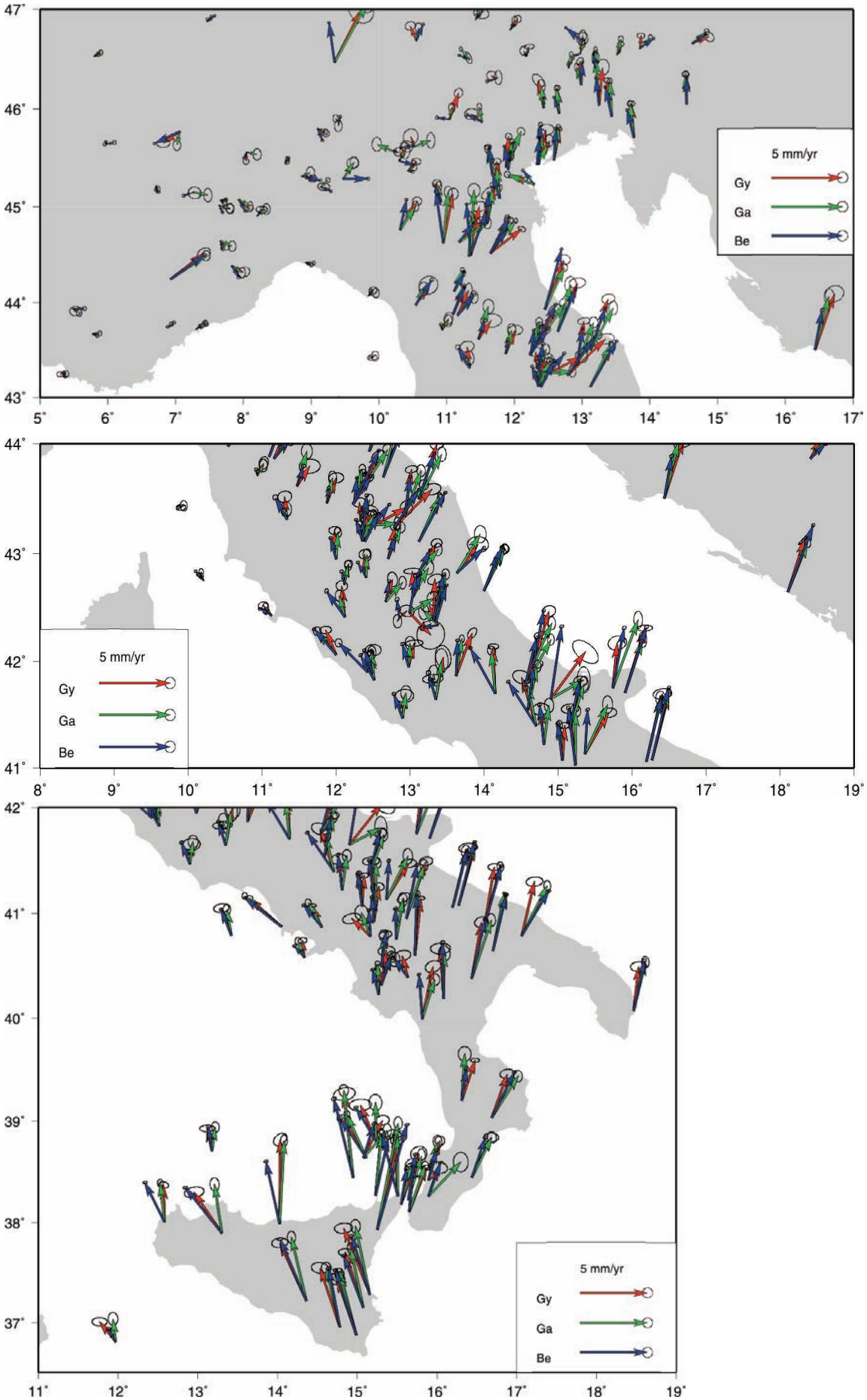

Figure 5. Comparisons among the GPS velocity fields carried out by the three different solutions for: a) northern; b) central; and c) southern Italian regions. The three solutions include only the common sites (217) with an observation interval longer than 2.5 years.

Id	Lat	Lon	W	Smax	Smin	Az	Sw	E	N
Be	54.847	-95.724	0.266	0.1	0.0	46.3	0.002	0.25	0.39
Ga	54.230	-99.430	0.253	0.1	0.1	42.0	0.001	0.40	0.29
Gy	54.875	-98.603	0.257	0.4	0.1	45.3	0.001	0.40	0.36

Be = Bernese; Ga = Gamit; Gy = Gipsy; Pole Coordinates (Lon., Lat. in degrees); Rotation rate (W, in °/Myr) and associated 1-sigma uncertainty (Sw); Semiaxes of the error ellipses (Smax, Smin); Azimuth of the Smax (Az). Also shown are the RMS residuals (in mm) of the horizontal components (E, N).

Table 2. Parameters of the Eulerian poles for the Eurasia reference frame obtained by the Bernese, GAMIT and Gipsy solutions.

ITRF2000 and recent ITRF2005 poles [Fernandes et al. 2003, Kreemer et al. 2003, D'Agostino and Selvaggi 2004, Serpelloni et al. 2005, Altamimi et al. 2007]. The mean post-fit residuals are 0.25mm/yr and 0.39mm/yr for the East and North components respectively. A few central European sites, including POTS, BOR1, LAMA and JOZE, are rejected, both at the 95% and 99% significance levels. Their uncertainties are probably underestimated in the ITRF2005, and may need to be reassessed in a future ITRF realization. All of the Siberian sites are rejected from being rigidly connected to central Europe, east of ARTU (58° E), and they have a 2-3 mm/yr W-ward residual velocity.

GAMIT data-processing strategy

Code and phase data from more than 780 continuous GPS stations that operate in the Euro-Mediterranean and African regions (Figure 4b) were analyzed with the GAMIT software (version 10.33), for the time interval 1998.0-2009.5, and following standard procedures for regional networks [e.g., Dong et al. 1998, McClucsky et al. 2000, Serpelloni et al. 2006].

We divided the whole network into twenty sub-networks, using fifteen stations in common to each sub-network. The sub-networking was performed following the original CGPS network configuration, to allow for the production of single daily loosely constrained solutions (including SINEX files) for each individual network, and to account for differences in the network data availability over time. Moreover, considering that in a later step our solutions are combined with global and regional loosely constrained solutions provided by the Scripps Orbit and Permanent Arrays Center (SOPAC; http://sopac.ucsd.edu), the original rinex data of stations already included in the SOPAC solutions are not re-analyzed if they are not among the fifteen common stations. The twenty sub-networks were analyzed on a 16-node Linux cluster [Serpelloni et al. 2009].

Our data analysis scheme to go from raw data to ground velocities, is divided into three main steps: 1) the code and phase data analysis (using GAMIT); 2) the combination of solutions; and 3) the position time-series analysis, including noise characterization. The post-processing steps, points 2) and 3), are performed with the QOCA software [Dong et al. 1998, Dong et al. 2002; available at http://gipsy.jpl.nasa.gov/qoca] and the CATS software [Williams 2008].

GAMIT uses double-differenced, ionosphere-free, linear combinations of the *L*1 and *L*2 phase observations, to generate weighted least-squares solutions for each daily session [King et al. 1985, Bock et al. 1986, Schaffrin and Bock 1988, Dong and Bock 1989]. An automatic cleaning algorithm [Herring et al. 2006] is applied to post-fit residuals, to repair cycle slips and to remove outliers. The effects of solid-earth tides, polar motion and oceanic loading are taken into account according to the IERS/IGS standard 2003 model [McCarthy and Petit 2004].

The estimated parameters for each daily solution include the three-dimensional Cartesian coordinates for each site, the six orbital elements for each satellite (semi-major axis, eccentricity, inclination, longitude of ascending node, argument of perigee, and mean anomaly), Earth orientation parameters (pole position and rate, and UT1 rate), and integer phase ambiguities. The atmospheric propagation delay is modeled by means of the Global Mapping Function (GMF) models of Boehm et al. [2006], which introduce longitude, latitude and time-of-year dependence of the older Niell Mapping Functions (NMFs) [Niell 1996], and which results in the highest accuracies in the vertical studies [Herring et al. 2006].

Since the wet contribution to atmospheric delay is poorly modelled using surface meteorological data, hourly piece-wise linear atmospheric zenith delays are also estimated at each station to correct the poorly modeled troposphere, along with three east-west and north-south atmospheric gradients per day, to allow for azimuth asymmetry; the associated error covariance matrix is also computed and saved. The elevation cutoff is set to 10° and we use the IGS absolute elevation dependent tables for modelling the effective phase centre of the receiver and satellite antennae. A full re-analysis of the whole data-set with the IGS05 orbits and the absolute phase center model has been completed from 2000 to the present.

In the second step, our loosely constrained solutions (GAMIT ascii «h-files») are combined with the SOPAC global and regional loosely constrained solutions using the ST_FILTER software [Dong et al. 2002] developed at the JPL. The ST_FILTER is run under the Portable Batch System

[Serpelloni et al. 2009], thus making daily combinations very fast (about 2-3 min per day). In particular, we combine our solutions with all of the six IGS sub-networks, and the Euref (EURA) and Eastern Mediterranean (EMED) h-files available from SOPAC. This combination brings to the total to about 800 stations that are available for the final combined solution. The ST_FILTER uses common stations and orbital parameters that are recorded in the GAMIT h-files, to align each solution to a reference precise global orbit, available from SOPAC, and to the ITRF (or IGS), adopting the internal-constraint approach [Dong et al. 1998, Dong et al. 2002]. A seven-parameter transformation (three network rotations, three network translations, and one scaling parameter) is performed, which aligns each daily solution to the IGS05 frame and to the GPS realization of the ITRF2005 reference frame [Altamimi et al. 2007]. All of the IGS core sites are initially used to compute the transformation parameters, and a maximum number of five iterations are performed to find the best set of IGS sites that better define the global reference-frame. In this step, offsets of the IGS-core sites due to earthquakes and/or station configuration changes are corrected using values obtained in a preliminary run, using *a-priori* values from SOPAC.

In the third step, position time series are analyzed to simultaneously estimate the secular term (i.e., the linear velocity), the offsets in the time series, and the seasonal terms (i.e., annual and semiannual seasonal terms). Residual time series (where bias, velocity, jumps and seasonal terms are removed) are later analyzed with the CATS software [Williams 2008], to estimate the noise characteristics of the time series, assuming a white+flicker noise error model. Velocity uncertainties are then rescaled based on the analysis of the noise at individual stations.

Gipsy/OASIS data-processing strategy

Code and phase data from about 730 CGPS sites for the time interval 1996.0-2009.7 have been processed with the Gipsy-Oasis II software from the NASA JPL [Lichten and Borders 1987]. These sites are located either in Italian regions (about 350 of them) or in the surrounding areas (about 380 of them) (Figure 4c).

Point positioning [Zumberge et al. 1997] and precise orbits and clocks from the JPL (http://sideshow.jpl.nasa.gov) were used to analyze the GPS data, followed by integer

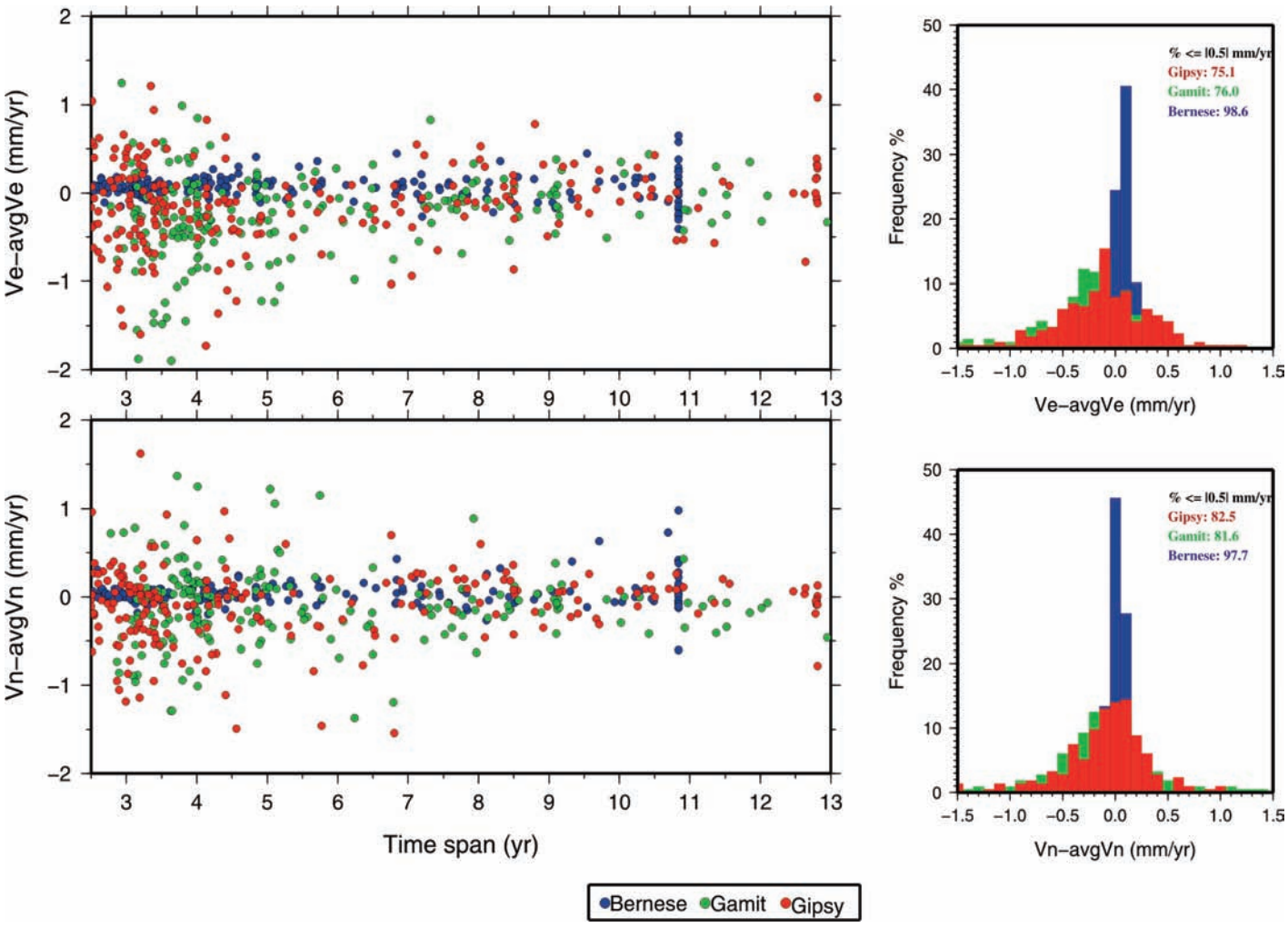

Figure 6. Left: Evolution of the velocity differences obtained between each solution and the AVF (*ΔV*, see text), with the time-span of each common site. Right: *ΔV* frequency distributions for the different solutions.

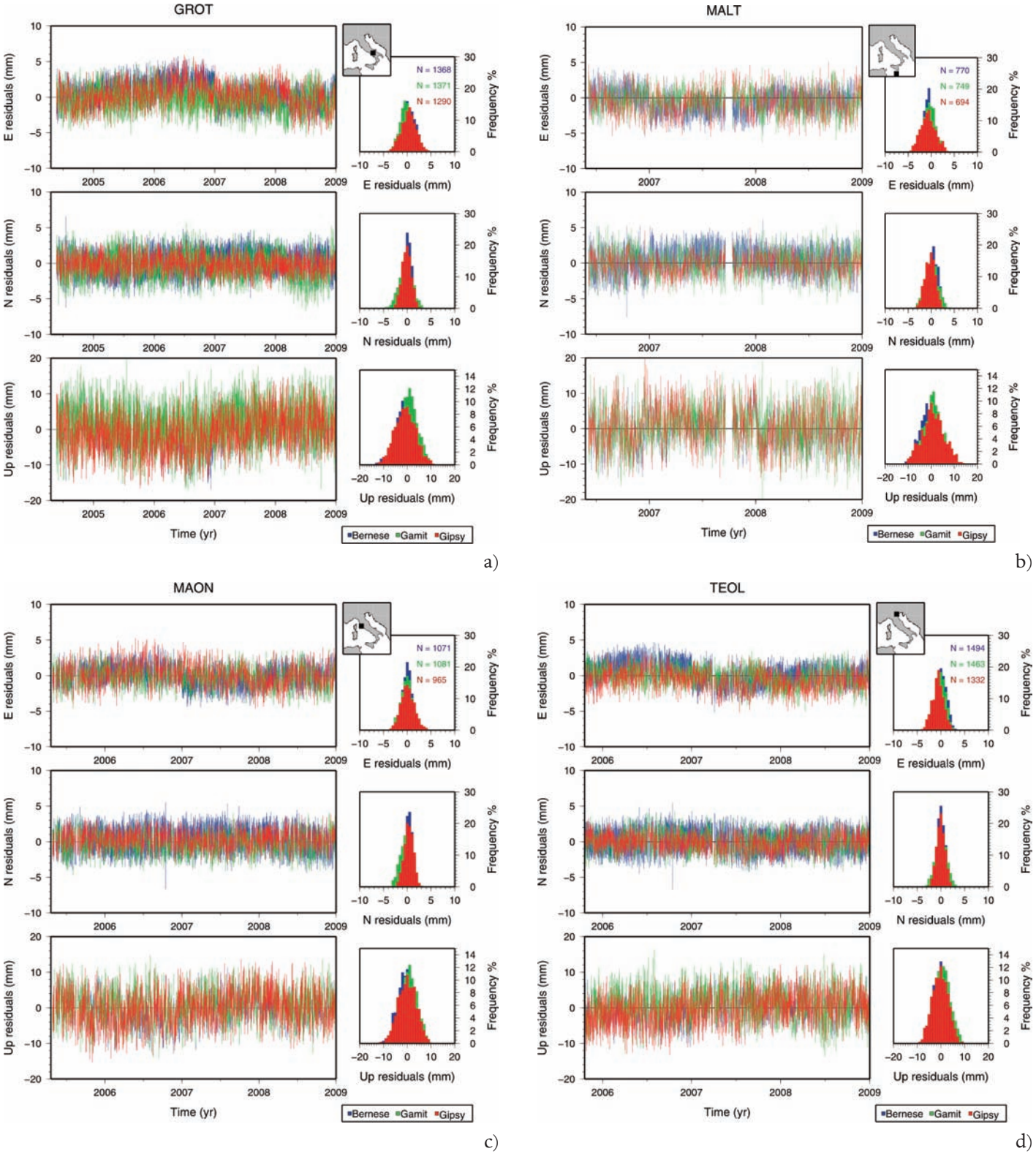

Figure 7. Comparisons for some of the RING sites of the residuals time series for the different softwares (left) and the relative RMS distributions (right) for which the number of samples is also given: a) GROT, Grottaminarda; b) MALT, Malta; c) MAON, Monte Argentario; d) TEOL, Teolo; e) USIX, Ustica.

ambiguity resolution. GPS ambiguity resolution of large amounts of data presents a serious challenge in terms of processing time. This step was performed using the Ambizap strategy [Blewitt 2008], to obtain unique, self-consistent daily ambiguity fixed solutions for the entire network. The Ambizap processing algorithm uses a fixed point theorem to identify linear combinations of network parameters that are theoretically invariant under ambiguity resolution [Blewitt 2008]. This strategy allows for very rapid and multiple re-analysis of large networks to assess various models, makes trivial the addition of extra stations of sub-networks to an existing solution, and produces unique, self-consistent daily ambiguity fixed solutions for the entire network.

Each ambiguity fixed daily solution is aligned to the

ITRF2005 reference frame [Altamimi et al. 2007] using a seven-parameter transformation. The realization of ITRF2005 is obtained using daily precise-point positioning solutions for about 92 stations in Eurasia, Nubia and the central Mediterranean, which are characterized by the longest observation intervals and minimum hardware changes, along with parameters from the JPL (x-files) that allow daily coordinate transformation into ITRF2005. A no-net rotation constraint was applied using a subset of 32 sites within the stable Eurasian continent that were deemed to be sufficiently far from tectonic and horizontal glacial isostatic adjustment effects [Nocquet et al. 2005]. After application of the no-net-rotation constraint, the RMS of the horizontal residual velocities of these 32 sites were 0.40 and 0.36 mm/yr for the East and North components, respectively. The rotational constraint was then applied to the 92-station frame, and transformation files (x-files) were then generated to transform daily non-fiducial solutions into a stable Eurasian reference frame. In this case, the temporal variation of the positions thus represents crustal motion relative to the stable Eurasian plate in the north (latitude), east (longitude) and vertical components.

The time series for all of the stations in the Eurasian reference frame (or in ITRF2005, and then locally rotated to NEU components) are cleaned from outliers using the strategy described in Nikolaidis [2002]. They are then analyzed for their noise properties, linear velocities, periodic signals and antenna jumps, using Maximum Likelihood Estimation (MLE). This technique allows simultaneous estimations of the noise properties structure together with the parameters of a time-dependent model of the data. The quantities estimated in the MLE analysis are linear trend, offsets at designated times, annual and semi-annual periodic signals and spectral law noise index and amplitude [Williams 2003]. The MLE analysis is performed using the CATS software [Williams 2008], and all of the parameters are estimated with white+flicker error models. Their uncertainties can thus be considered to be realistic estimates based on the analysis of the noise at individual stations.

Comparisons of the GPS solutions

In this study, we performed comparisons of the differently obtained GPS solutions on two different scales: 1) a regional scale comparison, which considers the discrepancies between each GPS velocity field; and 2) a more local scale comparison, which considers the differences in the residual time series for some particular CGPS sites. In these comparisons, which were performed only on the horizontal components of the GPS velocities, we took into consideration only the stations with an observation period longer than 2.5 years, given that shorter intervals might result in biased estimates of linear velocities [Blewitt and Lavallée 2002].

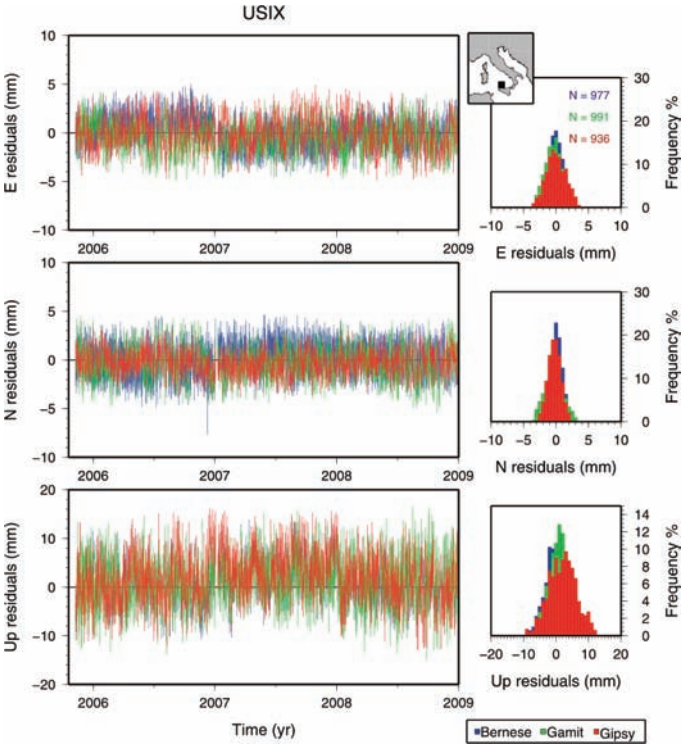

e)

Figure 7e. Caption on previous page.

Regional scale comparison

The Bernese, Gamit and Gipsy GPS velocity solutions used in this study include different numbers of sites (from ~370 to ~590). Also, the definition of the three Eurasian reference frames is significantly different (Figure 4a-4c): the Gamit solution does not use GPS sites to the west of the Rhine graben, but it uses several stations also in central Eurasia, whereas both the Gipsy and the Bernese solutions are mainly concentrated in Europe, from Spain to eastern Europe. On the other hand, despite these differences, the determinations of the Eulerian poles of the differently defined Eurasian plates relative to ITRF2005 are very similar (Figure 4d; Table 2). This aspect confirms the good quality of many of the CGPS stations in the Eurasia region.

The GAMIT and Gipsy solutions include points on the African plate. Thus, we determined the Africa poles with respect to Eurasia for these two solutions and we compared them with the previously GPS-derived Africa-Eurasia poles [Sella et al. 2002, Calais et al. 2003, Kreemer et al. 2003, McClusky et al. 2003, Serpelloni et al. 2007, D'Agostino et al. 2008]. Table 3 shows that Eulerian poles parameters of a Nubia reference frame with respect to Eurasia together with the previously mentioned solutions. In the comparison, we also inlcuded the Africa-Eurasia pole proposed by Nuvel1A [De Mets et al. 1994], obtained averaging the plates motion over the last 3Ma. The agreement of our solutions with the other GPS-derived solutions and their significant discrepancy with respect to the Nuvel1A Africa-Eurasia pole [De Mets et al. 1994] support the hypothesis of a post-3Ma change in relative plate motion between Africa (Nubia) and Eurasia [McClusky

Reference	Lat	Lon	W	Smax	Smin	Az	Sw
Nuvel1A	21.0	-20.6	0.120	6	0.7	-4.0	0.020
SEL02	-18.2	-20.1	0.062	9.5	3.7	-17.0	0.005
CA03	-10.3	-27.7	0.063	10.3	3.3	52.0	0.004
KR03	1.1	-21.3	0.060	6.9	5.8	21.0	0.010
MC03	-1.0	-21.5	0.060	4.8	4.3	0.0	0.005
SER07	-1.0	-15.9	0.068	2.2⋆	2.6⋆	n.d.	0.003
DA08	-8.7	-30.8	0.049	3.4	2.6	22.4	0.001
GAMIT	-0.9	-26.1	0.062	1.8	1.4	27.3	0.001
GIPSY	-8.7	-28.5	0.049	1.8	1.3	15.8	0.001

Nuvel1A = De Mets et al. 1994; SEL02 = Sella et al. 2002; CA03 = Calais et al. 2003; KR03 = Kreemer et al. 2003; MC03 = McClusky et al. 2003; SER07 = Serpelloni et al. 2007; DA08 = D'Agostino et al., 2008; GAMIT = the present study; Gipsy = the present study; Pole Coordinates (Lon., Lat. in degrees); Rotation rate (W, in °/Myr) and associated 1-sigma uncertainty (Sw); Semiaxes of the error ellipses (Smax, Smin); Azimuth of the Smax (Az). Star (⋆) indicates pole uncertainty expressed in the north and east components, instead of Smax and Smin. n.d. = not-determined in the study.

Table 3. Parameters of the Eulerian poles for the Nubia reference frame with respect to Eurasia obtained by the GAMIT and Gispy solutions and their comparison with previous studies.

et al. 2003, Calais et al. 2003, D'Agostino et al. 2008].

To determine whether the differences in the analyses affect the relative solutions that produce significant differences in the GPS velocity fields, we proceeded in three steps: 1) we defined an Average Velocity Field (AVF); 2) we compared the three solutions to the AVF; 3) we rotated the three solutions with respect to the AVF.

Despite the small number of different velocity solutions (three), and using only the 217 CGPS sites that are common to the three solutions, the AVF was calculated according to the site by site mean of the Eurasia-fixed velocity values for each horizontal component. This mean was weighted by the relative velocity uncertainties, the covariance, and the correlation indexes between the horizontal components. However, as the GPS velocity uncertainties have been calculated in different ways, to perform a rigorous comparison these uncertainties and covariances will probably need to be rescaled to avoid miscomputing of the AVF. Bianco et al. [2003] showed that knowing the χ_i^2 factor for each solution *i*, which corresponds to the ratio between the chi² value and the number of degrees of freedom (i.e. chi²/dof), it is possible to impose the following equation:

$$\sum \chi_i^2 = 1$$

to equally balance each solution contribution and to estimate the relative scaling factors. The scaling factors obtained for the Bernese and Gipsy solutions appear to be closer (5.58 and 5.41, respectively) than that obtained for the GAMIT solution (8.49). Finally, we again determined the weighted mean for the AVF, but with weighting also by the scaling factors computed in this way.

The original, un-rotated, results of the three independent analyses are plotted in Figure 5a-c and listed in Table SM1-3 (Supplementary Material). In the Supplementary Material also the AVF results (Table SM4) are reported. It is clearly evident that, at a first order inspection, no important differences in the regional velocity field can be recognized. Furthermore, a few sites have GPS velocity vectors that are clearly not coherent with respect to the neighbour velocity vectors and it is worth noting that the three solutions show the same incoherent aspects, thus strongly suggesting probable local site instabilities. On the other hand, in a few cases, one solution diverges significantly from the two other solutions. This aspect could be related to slight differences, in the analysis strategies, for the estimations of the offsets occurred at those sites (due to instrumental changes) or of the annual or semiannual signals in the time series (Table 1), thus providing differences in the velocities in the visually checked noisiest sites. However, these discrepancies represents few exceptions (< 7%) of a regionally coherent velocity field.

The consistency of the three velocity field has been also evaluated quantitatively. For each site and for each horizontal component, we computed the differences between each velocity solution and the AVF (ΔV). The RMS values of these residuals are summarized in Table 4. Then, we first plotted the ΔV values for both the horizontal components, with respect to the time-span of each AVF site (Figure 6, left), to determine whether these differences can be amplified, in any way, for young GPS sites. Indeed, Figure 6 shows that the largest ΔV cluster, which ranges from 0 to 1.5 mm/yr, is observed for the CGPS sites with an observation time-span lower than 3.5 yr. For sites with a life-span greater than 3.5 yr,

most of the ΔV values are below 0.5 mm/yr. Then, we plotted the residuals frequency distribution to quantify most of the discrepancies between the three different solutions and the AVF. This distribution shows that intrinsic discrepancies range between 0.1 mm/yr and 0.5 mm/yr, with an average value of 0.3 mm/yr (Figure 6, right).

Finally, we rotated each velocity solution with respect to the AVF. The RMS values resulting from each rotation (Table 4) for both of the horizontal components are very similar to those carried out in the previous step (i.e. before rotation).

From the results from either the simple differences between each pair of solution or the velocity field rotations, we can infer that there are no evident and systematic differences in the three solutions, and that only intrinsic differences among the three velocity solutions are seen. These intrinsic differences can be quantified in values of about 0.25-0.3 mm/yr for both of the horizontal components. This result is the first important evidence of the consistency of the differently defined GPS velocity fields in the area of the central Mediterranean plate boundary zone.

Site-scale comparisons

After the regional scale comparisons, we performed a more local comparison on some particular CGPS sites belonging to the RING network, in terms of their time series.

The time series available from the three solutions were produced in three different ways: the Bernese solution used the method proposed by Bianco et al. [2003]; the GAMIT solution adopted the method described by Dong et al. [2002]; whereas the Gipsy solution used the CATS software proposed by Williams [2008]. To rigorously compare the time-series results, we used the same type of analysis, using the CATS software, for most of the sites that are common to the three solutions. This was performed for the time interval ranging from the first epoch of the sites to their epoch 2009.0, which corresponds to our shortest investigated time-span solution (i.e. the Bernese one).

We have essentially applied the same approach as that previously described for the cases of the Gipsy solution, and we compared for each site the time series of residuals with respect to their nominal position. Thus, we have estimated in the MLE analysis the linear trend, the offsets at designated epochs, the annual and semi-annual periodic signals and the spectral law noise index and amplitude [Williams 2003]. All of the parameters are estimated adopting a white+flicker error model.

In Figure 7a-e, the comparison of the residual time series is associated with the comparison of the residuals frequency distribution in the three different solutions. The number of samples for each solution is also indicated. On one hand, the residuals time series are very similar and in most of the cases we can recognize the same periodic signals.

Cases	Common sites	Before Rotation RMS		After Rotation RMS	
		E	N	E	N
Be - AVF	217	0.14	0.15	0.13	0.12
Ga - AVF	217	0.49	0.48	0.49	0.49
Gy - AVF	217	0.48	0.48	0.49	0.49

Be, Bernese; Ga, Gamit; Gy, Gipsy; AVF, Average Velocity Field
The RMS residuals of the horizontal components (E, N) are shown.

Table 4. Comparison of the RMS values for the East and North velocity components before and after applying the rotation of each solution with respect to the Average Velocity Field.

On the other hand, some interesting discrepancies can be distinguished in the residuals frequency distributions. The residuals distributions for the North components are very similar, whereas for the East component the Bernese solution appears to be always more peaked than the others, with the distribution peak very close to the 0 value. About the vertical component, these discrepancies disappear. The Gipsy residuals distributions always appear to show a slightly smoother Gaussian distribution than the two other solutions. In general, we can infer that the three solutions are very close also at a local scale, i.e. the site scale.

Conclusions

In the present study, we have first described in detail the technologically advanced characteristics of the high-quality INGV CGPS infrastructure, as the RING network, and the impact for geophysical studies that is provided by such a dense national-scale CGPS network that is enlarged by other more local CGPS networks in Italy.

To really establish and evaluate the robustness of all of these CGPS networks in the central Mediterranean, we have described the different strategies adopted by the three data analyses. Despite the differences between the processing strategies, the comparisons show very good agreement both at the scale of the whole velocity field and at the scale of the particular site. Indeed, in the first case, we noted that the velocity discrepancies (RMS) among the three solutions do not exceed the RMS value of 0.3 mm/yr, whereas, in the second case, the differences in the distributions of the residuals in the position time series appear to be mostly on the East component.

The new increased number of CGPS stations now available allows more and more detailed spatial and temporal resolutions of the ongoing crustal deformation with respect to previous studies [Anzidei et al. 2001, Oldow et al. 2002, Caporali et al. 2003, Hollenstein et al. 2003, Nocquet and Calais 2003, Pondrelli et al. 2004]. This is confirmed by the robust improvements in the velocity field provided by more recent studies [Serpelloni et al. 2005, D'Agostino et al. 2008, Devoti et al. 2008] of plate boundary deformation in the central Mediterranean area.

Finally, the present study has highlighted the importance and the richness that the INGV represents, where different analysis groups are working with the three main geodetic-quality softwares.

Acknowledgements. We thank the staff of the INGV Grottaminarda Observatory and all the other INGV technicians who have tirelessly installed, and currently maintain, the RING network. Furthermore, we thank all of the agencies that have made the GPS observations that are used in this study available. The RING network was partially funded by the Italian Ministry for University and Research (MIUR) through the «Programma per la Sismologia e l'Ingegneria Sismica» (PROSIS) and partially funded by the Italian Civil Protection Department. R. D. acknowledges the Civil Defence Department Project S1-UR1.04. We also thank the Associate Editor and the two anonymous reviewers for constructive observations, which helped to increase the quality of the manuscript.

References

Altamimi, Z., X. Collilieux, J. Legrand, B. Garayt and C. Boucher (2007). ITRF2005: A new release of the International Terrestrial Reference Frame based on time-series station positions and Earth Orientation Parameters, J. Geophys. Res., 112, B09401, doi:10.1029/2007JB004949.

Anderson, H. and J. Jackson (1987). Active tectonics of the Adriatic region, Geophys. J. R. Astr. Soc, 91, 937-983.

Anzidei, M., P. Baldi, G. Casula, A. Galvani, E. Mantovani, A. Pesci, F. Riguzzi and E. Serpelloni (2001). Insights into present-day crustal motion in the central Mediterranean area from GPS surveys, Geophys. J. Int., 146, 98-110.

Anzidei M., P. Baldi and E. Serpelloni (2008). The coseismic ground deformations of the 1997 Umbria-Marche earthquakes: a lesson for the development of new GPS networks, Annals of Geophysics, 51, 27-43.

Battaglia, M., M. H. Murray, E. Serpelloni and R. Bürgmann (2004). The Adriatic region: An independent microplate within the Africa–Eurasia collision zone, Geophys. Res. Lett., 31, L09605, doi:10.1029/2004GL019723.

Beutler, G. et al. (2007). Bernese GPS Software, edited by R. Dach, U. Hugentobler, P. Fridez and M. Meindl, Astronomical Institute, University of Bern (January 2007).

Bianco, G., R. Devoti and V. Luceri (2003). Combination of loosely constrained solutions, IERS Tech. Note 30, 107-109.

Blewitt, G. (2008). Fixed-point theorems of GPS carrier phase ambiguity resolution and their application to massive network processing: Ambizap, J. Geophys. Res., 113, B12410, doi:10.1029/2008JB005736.

Blewitt, G. and D. Lavallée (2002). Effect of annual signals on geodetic velocity, J. Geophys. Res., 107 (B7), 2145, doi:10.1029/2001JB000570.

Bock, Y., S.A. Gourevitch, C.C. Counselman III, R.W. King and R. I. Abbot (1986). Interferometric analysis of GPS phase observations, Manuscripta Geodetica, 11, 282-288.

Boehm J., A. Niell, P. Tregoning and H. Schuh (2006). Global Mapping Function (GMF): A new empirical mapping function based on numerical weather model data, Geoph. Res. Lett., 33, L07304, doi:10.1029/2005/GL025546.

Calais, E., C. DeMets and J.M. Nocquet (2003). Evidence for a post-3.16-Ma change in Nubia-Eurasia-North America plate motions, Earth Planetary Science Letters, 216 (1-2), 81-92, doi:10.1016/S0012-821X(03)00482-5.

Calais, E., J.M. Nocquet, F. Jouanne and M. Tardy (2002). Current strain regime in the Western Alps from continuous Global Positioning System measurements 1996–2001, Geology 30 (7), 651-654.

Caporali, A., S. Martin and M. Missironi (2003). Average strain rate in the Italian crust inferred from a permanent GPS network-II. Strain rate versus seismic and structural geology, Geophys. J. Int., 155 (1), 254, doi:10.1046/j.1365-246X.2003.02035.x.

Cecere, G. (2007). La piattaforma tecnologica di gestione dati e informazioni della Rete Integrata Nazionale GPS (RING), Rapporti Tecnici INGV, 52.

Chiarabba C., L. Jovane and R. Di Stefano (2005). A new view of Italian seismicity using 20 years of instrumental recordings, Tectonophysics, 395 (3-4), 251-268.

D'Agostino, N., A. Avallone, D. Cheloni, E. D'Anastasio, S. Mantenuto and G. Selvaggi (2008). Active tectonics of the Adriatic region from GPS and earthquake slip vectors, J. Geophys. Res., 113, B12413, doi:10.1029/2008JB005860.

D'Agostino, N. and G. Selvaggi (2004). Crustal motion along the Eurasia-Nubia plate boundary in the Calabrian Arc and Sicily and active extension in the Messina Straits from GPS measurements, J. Geophys. Res., 109, B11402, doi:10.1029/2004JB002998.

D'Ambrosio, C. (2007). Variazione costruttiva applicata a monumentazioni, del tipo «Short-Drilled Braced», per stazioni GPS permanenti, Rapporti Tecnici INGV, 46.

De Mets, C., R. G. Gordon, D. F. Argus and S. Stein (1994). Effect of recent revisions to the geomagnetic time scale on estimates of current plate motions, Geophys. Res. Lett., 21, 2191-2194.

Devoti R., F. Riguzzi, M. Cuffaro and C. Doglioni (2008). New GPS constraints on the kinematics of the Apennines subduction, Earth Planet. Sci. Lett. 273, 163-174.

Dong, D and R. W. Bock (1989). GPS network analysis with phase ambiguity resolution applied to crustal deformation studies in California, J. Geophys. Res., 94, 3949-3966.

Dong, D., P. Fang, Y. Bock, M. K. Cheng and S. Miyazaki (2002). Anatomy of apparent seasonal variation from GPS-derived site position, J. Geophys. Res., 107, doi:10.1029/2001JB000573.

Dong, D., T. A. Herring and R. W. King (1998). Estimating regional deformation from a combination of space and terrestrial geodetic data, J. Geod., 72, 200-214.

Ekstrom, G. and P. England (1989). Seismic strain rates in regions of distributed continental deformation, J. Geophys. Res., 94, 10231-10257.

Estey, L.H. and C.M. Meertens (1999). TEQC: the multi-

purpose toolkit for GPS/GLONASS data, GPS solutions, 3 (1), 42-49, doi: 10.1007/PL00012778.

Falco, L. (2008). Implementazione e gestione di una rete di monitoraggio GPS e sismica mediante tecnologie GPRS/EDGE/UMTS/HSDPA, Rapporti Tecnici INGV, 69.

Fernandes, R.M.S., B.A.C. Ambrosius, R. Noomen, L. Bastos, M.J.R. Wortel, W. Spakman and R. Govers (2003). The relative motion between Africa and Eurasia as derived from ITRF2000 and GPS data, Geophys. Res. Lett., 30 (16), 1828.

Goes, S., D. Giardini, S. Jenny, C. Hollenstein, H.-G. Kahle and A. Geiger (2004). A recent tectonic reorganization in the south-central Mediterranean, Earth Planet. Sci. Lett., 226, 335-345.

Herring T.A., R.W. King and S.C. McClusky (2006). GPS Analysis at MIT, GAMIT Reference Manual, Release 10.3. Department of Earth, Atmospheric and Planetary Sciences, Massachusetts Institute of Technology, Cambridge MA (http://chandler.mit.edu/~simon/gtgk/GAMIT_Ref_10.3.pdf).

Hollenstein, C. H., H.-G. Kahle, A. Geiger, S. Jenny, S. Goes, and D. Giardini (2003). New GPS constraints on the Africa-Eurasia plate boundary zone in southern Italy, Geophys. Res. Lett., 30 (18), 1935, doi:10.1029/2003GL017554.

Jackson, J. & D. McKenzie (1988). The relationship between plate motions and seismic moment tensors, and the rates of active deformation in the Mediterranean and Middle East, Geophys. J. Int., 93, 45–73.

Kim, Y.J., A. Chaudhury and H.R. Rao (2002). A Knowledge Management Perspective to Evaluation of Enterprise Information Portals, Knowledge and Process Management, 9 (2), 57-71.

King, R.W., J. Collins, E.M. Masters, C. Rizos and A. Stolz (1985). Surveying with Global Positioning System, School of Surveying, University of New South Wales, Sydney, monograph n. 9.

Kreemer, C., W. E. Holt and A. J. Haines (2003). An integrated global model of present-day plate motions and plate boundary deformation, Geophys. J. Int., 154, 8-34.

Lichten, S. and J. Borders (1987). Strategies for High precision Global Positioning System Orbit Determination, J. Geophys. Res., 92, 12751-12762.

McCarthy, D. D. and G. Petit (2004). IERS Conventions 2003, IERS Technical Note 32, Verlag des Budesamts fur Kartographie und Geodasie, Frankfurt.

McClusky, S., S. Balassanian, A. Barka, C. Demir, S. Ergintav, I. Georgiev, O. Gurkan, M. Hamburger, K. Hurst, H.-G. Kahle, K. Kastens, G. Kekelidze, R. King, V. Kotzev, O. Lenk, S. Mahmoud, A. Mishin, M. Nadariya, A. Ouzounis, D. Paradissis, Y. Peter, M. Prilepin, R. Reilinger, I. Sanli, H. Seeger, A. Tealeb, M.N. Toksoz, and G. Veis (2000). Global Positioning System constraints on plate kinematics and dynamics in the eastern Mediterranean and Caucasus, J. Geophys. Res., 105 (B3), 5695-5719.

McClusky, S., R. Reilinger, S. Mahmoud, D. Ben Sari and A. Tealeb (2003). GPS constraints on Africa (Nubia) and Arabia plate motions, Geophys. J. Int., 155, 126-138.

Miyazaki, S., H. Tsuji, Y. Hatanaka, Y. Abe, A. Yoshimura, K. Kamada, K. Kobayashi, H. Morishita and Y. Imura (1994). Establishment of the nationwide HPS array (Grapes) and its initial results on the crustal deformation of Japan, Bullettin of the Geographycal Survey Inst., 42.

Niell A. (1996). Global mapping functions for the atmospheric delay at radio wavelenghts, J. Geoph. Res., 101, 3227-3246.

Nikolaidis, R. (2002). Observation of geodetic and seismic deformation with the Global Positioning System, PhD thesis, University of California, San Diego.

Nocquet, J.-M. and E. Calais (2003). Crustal velocity field of Western Europe from permanent GPS array solutions 1996-2001, Geophys. J. Int., 154, 72, doi:10.1046/j.1365-246X.2003.01935.x.

Nocquet, J.-M., E. Calais and B. Parsons (2005). Geodetic constraints on glacial isostatic adjustment in Europe, Geophys. Res. Lett., 32, L06308, doi:10.1029/2004GL022174.

Oldow, J. S., L. Ferranti, D. S. Lewis, J. K. Campbell, B. D'Argenio, R. Catalano, L. Carmignani, P. Conti and C.L.V. Aiken (2002). Active fragmentation of Adria, the north African promontory, central Mediterranean orogen, Geology, 30 (9), 779-782.

Pondrelli, S., C. Piromallo and E. Serpelloni (2004). Convergence vs. retreat in Southern Tyrrhenian Sea: Insights from kinematics, Geophys. Res. Lett., 31, L06611, doi:10.1029/2003GL019223.

Rebai, S., H. Philip and A. Taboada (1992). Modern tectonic stress field in the mediterranean region: evidence for variation in stress directions at different scale, Geophys. J. Int., 110, 106-140.

Schaffrin, B. and Y. Bock (1988). A unified scheme for processing GPS phase observations, Bull. Geodesique, 62, 142-160.

Sella, G. F., T. H.Dixon and A. Mao (2002). REVEL: a model for recent plate velocities from space geodesy, J. Geophys. Res., 107 (B4), doi:10.1029/2000JB000033.

Selvaggi, G., M. Mattia, A. Avallone, N. D'Agostino, M. Anzidei, M. Cantarero, V. Cardinale, A. Castagnozzi, G. Casula, G. Cecere, R. Cogliano, F. Criscuoli, C. D'Ambrosio, E. D'Anastasio, P. De Martino, S. Del Mese, R. Devoti, L. Falco, A. Galvani, L. Giovani, I. Hunstad, A. Massucci, F. Minichiello, A. Memmolo, F. Migliari, R. Moschillo, F. Obrizzo, G. Pietrantonio, M. Pignone, M. Pulvirenti, M. Rossi, F. Riguzzi, E. Serpelloni, U. Tammaro and L. Zarrilli (2006). La Rete Integrata Nazionale GPS (RING) dell'INGV: un'infrastruttura aperta per la ricerca scientifica, X Conferenza ASITA, Bolzano, Atti, II, 1749-1754.

Serpelloni, E., M. Anzidei, P. Baldi, G. Casula and A. Galvani (2005). Crustal velocity and strain-rate fields in Italy and surrounding regions: New results from the analysis of

permanent and non-permanent GPS networks, Geophys. J. Int., 161, 861–880, doi:10.1111/j.1365-246X. 2006.06218.x.

Serpelloni, E., G. Casula, A. Galvani, M. Anzidei and P. Baldi (2006). Data analysis of permanent GPS networks in Italy and surrounding regions: application of a distributed processing approach, Annals of Geophysics, 49 (4-5), 1073-1104.

Serpelloni, E., P. Perfetti and A. Cavaliere (2009), Progettazione e realizzazione di un computer-cluster per l'analisi dati GPS con i software GAMIT e QOCA, Rapporti Tecnici INGV, 93.

Serpelloni, E., G. Vannucci, S. Pondrelli, A. Argnani, G. Casula, M. Anzidei, P. Baldi and P. Gasperini (2007). Kinematics of the Western Africa-Eurasia Plate Boundary From Focal Mechanisms and GPS Data, Geophys. J. Int., doi: 10.1111/j.1365-246X.2007.03367.x.

Vannucci, G., S. Pondrelli, A. Argnani, A. Morelli, P. Gasperini and E. Boschi (2004). An Atlas of Mediterranean seismicity, Annals of Geophysics, 47 (1), Suppl., 247-306.

Westaway, R. (1990). Present-day kinematics of the plate boundary zone between Africa and Europe, from the Azores to the Aegean, Earth Planet. Sci. Lett., 96, 393-406.

Williams, S. D. P. (2003). The effect of coloured noise on the uncertainties of rates estimated from geodetic time series, J. Geod., 76, 483-494.

Williams, S. D. P. (2008). CATS: GPS coordinate time series analysis software, GPS solutions, 12 (2), 147-153, doi:10.1007/ s10291-007-0086-4.

Zhang, J., Y. Bock, H. Johnson, P. Fang, S. Williams, J. Genrich, S. Wdowinski and J. Behr (1997). Southern California Permanent GPS array: error analysis of daily positions estimates and site velocities, J. Geophys. Res., 102 (B8), 18035-18055.

Zumberge, J. F., M. B. Heflin, D. C. Jefferson, M. M. Watkins and F. H. Webb (1997). Precise point positioning for the efficient and robust analysis of GPS data from large networks, J. Geophys. Res., 102 (B3), 5005-5018.

*Corresponding author: Dr. Antonio Avallone, Istituto Nazionale di Geofisica e Vulcanologia, Centro Nazionale Terremoti, Roma, Italy; e-mail: antonio.avallone@ingv.it